Machine Learning Assisted Phase-less Millimeter-Wave Beam Alignment in Multipath Channels

Benjamin W. Domae, Ruifu Li, and Danijela Cabric

Electrical and Computer Engineering Department,
University of California, Los Angeles
bdomae@ucla.edu, doanr37@ucla.edu, danijela@ee.ucla.edu

Abstract—**Communication systems at millimeter-wave (mmW) and sub-terahertz frequencies are of increasing interest for future high-data rate networks. One critical challenge faced by phased array systems at these high frequencies is the efficiency of the initial beam alignment, typically using only phase-less power measurements due to high frequency oscillator phase noise. Traditional methods for beam alignment require exhaustive sweeps of all possible beam directions, thus scale communications overhead linearly with antenna array size. For better scaling with the large arrays required at high mmW bands, compressive sensing methods have been proposed as their overhead scales logarithmically with the array size. However, algorithms utilizing machine learning have shown more efficient and more accurate alignment when using real hardware due to array impairments. Additionally, few existing phase-less beam alignment algorithms have been tested over varied secondary path strength in multipath channels. In this work, we introduce a novel, machine learning based algorithm for beam alignment in multipath environments using only phase-less received power measurements. We consider the impacts of phased array sounding beam design and machine learning architectures on beam alignment performance and validate our findings experimentally using 60 GHz radios with 36-element phased arrays. Using experimental data in multipath channels, our proposed algorithm demonstrates an 88% reduction in beam alignment overhead compared to an exhaustive search and at least a 62% reduction in overhead compared to existing compressive methods.**

Index Terms—**beam alignment, mmW, machine learning**

I. INTRODUCTION

Due to large swaths of available bandwidth, upper mmW and sub-terahertz (sub-THz) are strong candidates for future high data rate cellular and wireless local area networks. To overcome the significantly higher path loss in these bands, mmW wireless systems must use strongly directional antenna patterns for data communication. User equipment (UE) typical requires phased array antennas with many elements to achieve electronically steerable directional beams. Additionally, during an initial connection to a base station (BS), initial access (IA), the UE receiver (Rx) must properly steer the phased array beam towards the BS transmitter (Tx). In current mmW systems, this directional beam selection method, commonly known as beam alignment (BA) or beam training, requires

synchronization signal correlation measurements for an exhaustive search over all possible Rx beam directions. Since antenna arrays with more elements generate narrower directional beams, BA communications overhead increases linearly with the array size. As future wireless systems at mmW and sub-THz frequencies require larger arrays for higher gain, exhaustive search BA may be impractical.

Accelerated BA is an active area of research, with prior work primarily using compressive sensing (CS) or machine learning algorithms verified through simulations. Other solutions to BA include hierarchical searches [1] [2]; algorithms utilizing out-of-band information, such as node locations [3] or sub-6 GHz channel information [4]; and designs requiring novel array architectures [5].

Several existing solutions apply CS methods to solve BA. [6] utilizes a matching pursuit (MP) algorithm with channel gain measurements from pseudorandom noise (PN) beams, quasi-omni-directional beams with random phase antenna weight vector (AWVs). [7] also employs MP with PN sounding beams, but only requires received signal strength (RSS) power measurements by solving phase-less BA as a compressive phase retrieval (CPR) problem. SBG-Code from [8] solves BA for hybrid or digital arrays as a CPR problem.

Machine learning methods have also been proposed for multipath or phase-less BA. [9] and [10] each study *sample-based* convolutional neural network (CNN) algorithms in multipath channels. As described later, sample-based IA may not be practical for high mmW IA. mmRAPID [11] and DeepIA [12] each only require phase-less RSS measurements from PN beams and pencil beams respectively, but do not thoroughly study the impact of multipath channels on the BA performance. Thus, none of these works address phase-less mmW BA performance over varied multipath strength.

Few prior works have experimentally validated their BA algorithms. [11] used a 60 GHz testbed but with only single path and line-of-sight (LOS) channels, while [13] experimentally studied multi-user beam steering at 60 GHz but did not evaluate machine learning based BA. [9] tested a sample-based CNN algorithm in a simple 60 GHz non-line-of-sight (NLOS) channel, but did not thoroughly investigate the impact of multipath strength. To the authors' best knowledge, this work is the first to experimentally verify a machine learning based phase-less BA algorithm at mmW in multipath channels.

In this work, we propose an alternative algorithm for BA to

reduce the communications overhead. We develop our system model and problem statement in Section II, then describe our proposed phase-less BA algorithm, including the foundation for this work in [11], in Section III. In Section IV, we discuss our evaluation of the algorithms, including 60 GHz experiments, simulations, and tradeoff results. Finally, we conclude in Section V.

Notation: Scalars, vectors, and matrices are represented by non-bold lowercase, bold lowercase, and bold uppercase letters respectively. The ith column of a matrix $\mathbf{A}$ is denoted as $[\mathbf{A}]_i$. The transpose and Hermitian transpose of $\mathbf{A}$ are $\mathbf{A}^T$ and $\mathbf{A}^H$ respectively. $|\mathbf{A}|$ denotes the entry-wise magnitude of $\mathbf{A}$.

II. System Model and Problem Statement

This section formally defines our system model, the phase-less BA problem, and limitations of existing solutions.

A. Multipath Channel Model

For our algorithm design and simulations, we consider a simplified mmW multipath channel model to provide a succinct metric for the relative strength of the NLOS paths. To simplify the path gains for the few significant angles-of-arrival (AoA), we use a geometrically decaying model where each distinct path is successively attenuated by $e^{-\alpha}$. The model parameter α describes the channel gain and the BS antenna response at the angle-of-departure (AoD) for each path. The channel is explicitly described in (1), where $[\mathbf{a}_R(\phi_l)]_n = a_n \exp(j2\pi(n-1)\sin(\phi_l)d/\lambda)$ is the nth element of the UE Rx array response and a_n is the complex coefficient representing element-wise hardware mismatch. Ideally, $a_n = 1$ for every element, but this is difficult to achieve in practice. Due to physical channel characteristics, even multipath and NLOS channels at mmW typically only feature a few strong paths [14]. In this work, we assume $L = 3$ for simulations and design experiments with $L \in \{2, 3\}$.

$$\mathbf{h} = \sum_{l=1}^{L} e^{-\alpha l} \mathbf{a}_R(\phi_l), \quad \mathbf{h} \in \mathbb{C}^{N_r} \quad (1)$$

B. Problem Statement: Phase-less Beam Alignment

This work addresses user BA with phase-less power measurements from a single, predefined sensing codebook. Phase-less measurements are specifically considered because devices generally have poor phase estimation during the early stages of IA. Commodity hardware, like the 60 GHz radios used in this work, do not support phase measurements during BA. Furthermore, the phase noise in hardware at upper-mmW and sub-THz frequencies would make phase information during BA unreliable [15]. We avoid algorithms with adaptive sensing codebooks (designs that change codebooks based on prior measurements, e.g. hierarchical searches) or out-of-band information to reduce the beam management circuit complexity.

Given a UE with N_r antennas, the sensing codebook with M measurements can be represented as $\mathbf{W}_s \in \mathbb{C}^{N_r \times M}$, while the codebook used for data communications with K directional beams is $\mathbf{W}_d \in \mathbb{C}^{N_r \times K}$. The BS is assumed to be transmitting a pilot sequence, either omni-directionally or

with a beam aligned to the user before UE BA. The phase-less measurements for a given channel $\mathbf{h}$ is then shown in (2).

$$\mathbf{y} = \left|\mathbf{W}_s^H \mathbf{h} s + \mathbf{W}_s^H \mathbf{n}\right|, \quad \mathbf{y} \in \mathbb{R}^M \quad (2)$$

The goal of BA is ultimately to find the best directional beam for data communication, as in $i = \arg\max_i \left|[\mathbf{W}_d]_i^H \mathbf{h} s\right|$. An estimated solution to this problem can be written as the objective for the traditional exhaustive search algorithm (4).

$$y_{d,i} = \left|[\mathbf{W}_d]_i^H \mathbf{h} s + [\mathbf{W}_d]_i^H \mathbf{n}\right| \quad (3)$$

$$\hat{i} = \arg\max_i y_{d,i}^2 \quad (4)$$

For algorithms using a non-adaptive sensing codebook, phase-less BA's objective is to estimate $\hat{i}$ using $\mathbf{y}$, as in (5). Since the true probability is difficult to estimate, compressive BA approximates $\tilde{i}$ with BA algorithm $p(\mathbf{y})$. On the other hand in an exhaustive search, $p(\mathbf{y}) = \arg\max_i y_i^2$ and $\mathbf{W}_s = \mathbf{W}_d$.

$$\tilde{i} = \arg\max_i P(i = \hat{i} \mid \mathbf{y}) \approx p(\mathbf{y}) \quad (5)$$

When designing $p(\mathbf{y})$, accuracy, gain loss, and number of required measurements serve as performance metrics. Since (5) represents a classification problem, the *accuracy* of $p(\mathbf{y})$ for N test points is the fraction of test points with the correct predicted beam direction: $acc(\hat{i}, p(\mathbf{y})) = \frac{1}{N}\sum_{j=1}^{N} \mathbb{1}[\hat{i} = p(\mathbf{y})]$. Accuracy, however, does not capture the impact of incorrect prediction on the data communication phase. In this work, the alignment quality is measured using maximum *gain loss* $g = \mathbb{E}[|y_{d,\hat{i}}|^2]/\mathbb{E}[|y_{d,p(\mathbf{y})}|^2]$, or the difference in gain (in dB) between the optimal pencil beam and the pencil beam selected by the BA algorithm, for a specified percentile of N predictions. To evaluate the effective reduction in overhead, this work uses the *required number of measurements* to meet a maximum gain loss requirement.

The goal of this work is thus to demonstrate a machine learning based $p(\mathbf{y})$ and alternative $\mathbf{W}_s$ that reduce the required number of measurements for BA in multipath channels.

C. Model-based Solutions and their Limitations

Phase-less CS algorithms commonly use MP with RSS measurements (denoted RSS-MP) from specially designed sounding beams as $p(\mathbf{y})$. [7] applies this method with quasi-omni-directional PN beams. PN beams use random phases for each antenna element, e.g. 2-bit phase AWV $[\mathbf{W}_s^{PN}]_i$ with nth entry $w_n = \exp(\phi_n), \phi_n \in \{0, \frac{\pi}{2}, \pi, \frac{3\pi}{2}\}$, creating random antenna patterns with low angular correlation between beams. Alternatively, the adaptive codebook and scoring system in [1] can be reformulated as an RSS-MP algorithm with multifinger beams with multiple directional lobes. In this work, these two MP algorithms are used as baselines for comparison.

Practical hardware and multipath channels provide challenges for phase-less, model-based BA performance. RSS-MP with PN beams rely on perfect prior knowledge of the dictionary, $\mathbf{W}_s^{PN}$, for good spatial reconstruction. [11] experimentally demonstrated that PN beam RSS-MP is vulnerable to poor array calibration and hardware impairments. Additionally, signals from different channel paths can interfere destructively in phase-less, compressive measurements,

compromising angular path distinction. In the noise-free case below, interference between different paths are included in the second summation, distorting the RSS measurement $|y_i|^2$.

$$
\begin{aligned}
|y_i|^2 = \;& \left| [\mathbf{W}_s]_i^H \, \mathbf{h} \right|^2 \\
= \;& \sum_l |\alpha_l|^2 \left| [\mathbf{W}_s]_i^H \, \mathbf{a_R}(\phi_{l_1}) \right|^2 + \\
& \sum_{l_1 \neq l_2} 2\mathcal{R}e \left\{ \alpha_{l_1}^H \alpha_{l_2} \mathbf{a_R}(\phi_{l_1})^H [\mathbf{W}_s]_i \, [\mathbf{W}_s]_i^H \, \mathbf{a_R}(\phi_{l_2}) \right\}
\end{aligned}
$$

To reduce magnitude of the second term, *sparsely supported* beams are necessary. Beams, $[\mathbf{W}_s]_i$, that are sparsely supported in the angular space only have large gain for few angles ϕ_l, reducing the probability of interference with other AoAs. [8] demonstrated this property with theoretical bounds on BA performance, while [1] utilized this principle with phased array multifinger beams. A simple numerical demonstration of the need for sparsely supported beams is given below. Suppose the channel $\mathbf{h} = \mathbf{W}_d^H \hat{\mathbf{x}}$ is on-grid for vector $\hat{\mathbf{x}} \in \mathbb{C}^K, \|\hat{\mathbf{x}}\|_0 = L$ representing a sparse set of paths with largest entry at index $\hat{\imath}$. Consider the following model-based algorithm that estimates $|\hat{\mathbf{x}}|$ by solving a phase-less version of MP (6).

$$
\begin{aligned}
\min_{\mathbf{x},\epsilon} \quad & \gamma \|\mathbf{x}\|_1 + \epsilon \quad\quad\quad\quad (6) \\
\text{s.t.} \quad & \left\| \left| \mathbf{W_s^H W_d} \right| \mathbf{x} - |\mathbf{y}| \right\|_2^2 \leq \epsilon \|\mathbf{y}\|_2^2, \\
& \mathbf{x} \succeq 0
\end{aligned}
$$

Here, $\mathbf{x}$ is an estimate of $|\hat{\mathbf{x}}|$, ϵ captures distortion in $\mathbf{y}$ due to interference between multipath components, and γ is a trade-off constant for the tolerance to ϵ. For each realization of the channel, this algorithm's performance is evaluated with two codebooks $\mathbf{W}_s$: PN beams $\mathbf{W}_s^{PN}$ and one containing sparse beams encoding all K on-grid angles from [8]. Fig. 1 shows the simulated accuracy, with $N_r = K = 72, M = \frac{N_r}{3} = 24, \gamma = 0.01$, under different channel sparsity $L \in \{1, 2, 3, 4\}$. To ensure convergence of ϵ, $|\mathbf{y}|$ is normalized by its maximum entry before using the CVX solver. The accuracy, $acc(\hat{\imath}, \tilde{\imath})$, compares $\hat{\imath}$ with predictions $\tilde{\imath} = \arg\max_i |\mathbf{x}|_i$. The PN codebook achieves a high accuracy in predicting AoA with no multipath components ($L = 1$), but degrades drastically with $L > 1$, requiring a relaxed ϵ to get a feasible solution. Performance of the sparse beams remains high even with $L = 4$ and an order of magnitude smaller ϵ, demonstrating that sparse beams are more consistent in multipath channels.
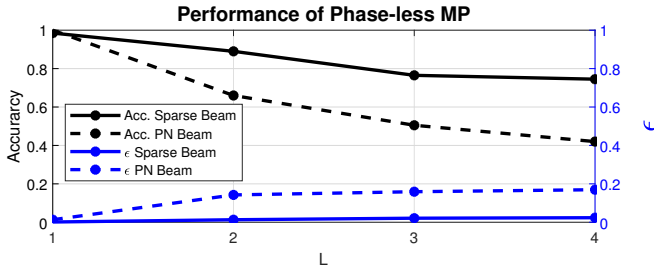

Fig. 1: MP performance vs. number of channel paths

III. ALGORITHM DESIGN

To reduce BA overhead in multipath channels, this paper proposes an improved version of mmRAPID [11]. Like mm-RAPID, the approach uses the same two-stage lifecycle and classification formulation to reduce the impact of hardware impairments. However, the proposed algorithm utilizes a novel combination of sounding beams and a CNN architecture to exploit correlation between the new features. This section provides insight into these design choices and tradeoffs.

A. Two-Stage Data-Driven Phase-less Beam Alignment

The two-stage machine learning (ML) algorithm design in mmRAPID serves as the foundation for this work. During the training stage, the UE conducts both an exhaustive search using the directional codebook $\mathbf{W}_d$ and the compressive measurements with the sensing codebook $\mathbf{W}_s$. After collecting sufficient data, the machine learning classification model is trained using the best directions as labels and the sensing measurements as features. In the ML architectures, this translates to an input layer of size M and an output score vector of size K. During the testing stage, the UE only uses $\mathbf{W}_s$ for BA sounding. Although the UE will see higher IA overhead during the training stage, the overhead is much smaller during the testing stage and the majority of device usage.

B. Sounding Beam Design

This work considers three heuristic beam designs for the sounding codebook $\mathbf{W}_s$: PN beams, sub-array (SA) multifinger beams, and single lobe quadratic phase distribution (QPD) beams. The PN beams in this work are defined with 2-bit phase (see Section II-C). As shown in Fig.1, PN beams are not ideal for phase-less multipath BA, thus the sparser multifinger beams and QPD beams are tested.

SA multifinger beams, abbreviated as SA beams, have multiple directional lobes with lower maximum gain than full pencil beams. As in [1], SA beam AWVs are generated by concatenating weight vectors for independently-steered pencil beams from single subsections of the phased array. Formally, the AWV for the ith sub-array, pointing toward θ_i, is $w_{i,n} = \exp(\phi_{1,n}), \phi_{i,n} = 2\pi n \sin(\theta_i)d/\lambda$.

QPD beams from [16] use phase adjustments to widen pencil beams using the entire phased array. Increasing design parameter $\Phi > 0$ increases the added phase $\phi_{n,qpd} = 4\Phi \times \left(\frac{2n-(N+1)}{2(N+1)}\right)^2$ and the beamwidth, but decreases the maximum gain. The overall AWV for a QPD beam pointing toward θ is $[\mathbf{W}_s^{QPD}]_{i,n} = \exp(\phi_n), \phi_n = 2\pi n \sin(\theta)d/\lambda + \phi_{n,qpd}$. This work assumes $\Phi = \pi$ for sparsely supported beams with the same beamwidth as an SA beam finger, but with higher gain.

C. Machine Learning Architecture

While the mmRAPID algorithm used a multi-layer perceptron (MLP) for ML based beam alignment, alternative algorithms may provide better AoA prediction. This work investigates CNNs to improve phase-less BA over MLPs. CNNs are commonly used in image processing for their ability
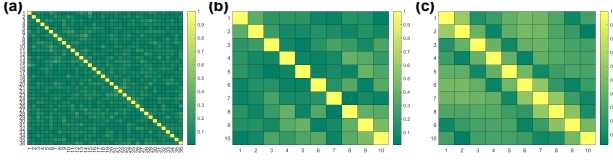
Fig. 2: Correlation between RSS features in a multipath channel. (a) PN beams; (b) SA beams; (c) QPD beams
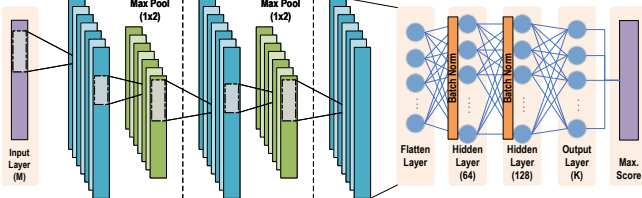

Fig. 3: CNN architecture considered

to utilize correlation in the feature space. Thus, if the RSS measurements from the sounding beams are correlated for a given channel, a CNN may improve performance. Data collected from the 60 GHz testbed, described in Section IV-A, show significant correlation in the feature space for SA and QPD beams. Fig. 2 shows the average experimental correlation found between features in a 2000 realizations of a multipath channel with $L = 2$ and $\alpha = 0.2$. This correlation encourages the study of CNNs as a potential prediction algorithm.

Fig. 3 details the tuned CNN architecture. The convolutional layers extract features for the following MLP. Note that the evaluated MLP prediction model is the same as the CNN's MLP stage, other than an input layer replacing the flatten layer. Both use ReLU activation functions for the outputs of layers and are trained with the RMSprop optimizer. As the algorithms aim to solve BA as a classification problem, both designs use sparse categorical cross entropy as a loss function. Both the MLP and CNN algorithms were developed in Tensorflow using the Keras API, with network hyperparameters selected using separate validation data from past experiments. *The code and dataset will be available upon publication.*

IV. ALGORITHM EVALUATION

A. Experimental Testbed

To capture the impact of practical hardware impairment, the algorithms were verified using a 60 GHz testbed featuring two Facebook Terragraph (TG) radios. Using IEEE 802.11ad
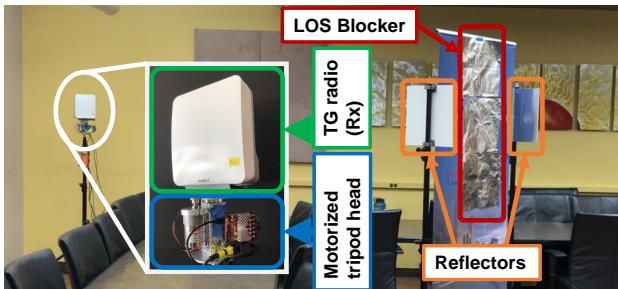

Fig. 4: Testbed Rx with two reflectors and a LOS blockage.

packet preambles, the TG radios measure received power and SNR estimates. Each TG radio features a 36×8 element phased array, with programmable phase in the 36 element horizontal axis. The programmable phase enabled measurements with custom azimuthal beamforming used in the sounding codebook design discussed in Section III-B.

The receiver TG radio was attached to a programmable motorized turntable, enabling the automated data collection required for the ML datasets. For a given channel environment with manually-placed reflectors, obstructions, and TG nodes, the software controls the radios and turntable to capture channel measurements with varied physical angles between the two phased arrays. Each new angle between the Tx and Rx geometrically provides a new channel configuration. Fig. 4 shows the Rx TG radio with the motorized turntable.

B. Simulation Design and Data Preparation

We created two separate datasets based on simulations and measurements. The simulations study a wider variety of multipath channels, while the experiments investigate hardware impairment impact. Even with automated collection, the number of experimental channels was limited by time constraints. The experimental data includes 8 α configurations, each with fixed relative separation between AoAs, rotated to 2000 different physical AoAs. However, the simulations include 9 α's, each with 10 measurements from 400 AoA relative separations, totaling 4000 channel realizations per α. Simulated paths were randomly selected over a $30°$ range, only requiring at least $2°$ of separation to maintain distinct AoAs.

Both simulated and experimental data are validated and split into separate training and testing sets. Each label used 144 samples for training, with the remaining data used for testing. With these fixed training set sizes, the simulated ML algorithms train with fewer examples of each AoA combination. Data validation removed points with labels without the required 144 training points. In this work, validation left $K = 54$ and $K = 51$ pencil beam labels (and maximum exhaustive search BA overhead) for simulations and experiments respectively.

C. Evaluation Results

This work empirically compares the discussed algorithms to find tradeoffs for $\mathbf{W}_s$ and $p(\mathbf{y})$ designs. Both simulations and experiments used the same $\mathbf{W}_d$ and $\mathbf{W}_s$, but no impairments were added in the simulations. $\mathbf{W}_d$ included 64 pencil beams over TG's supported angular range of $[-45°, 45°]$, oversampling the AoAs. For baseline methods, $\mathbf{W}_s^{PN}$ included 36, 2-bit PN beams. Each SA beam used three, 12-element virtual sub-arrays with $25°$ separation between fingers. Both SA and QPD codebooks include 10 beams with even angular separation ($9°$) between the centers of codes. Fig. 5 presents the theoretical and experimentally measured beam patterns of the one QPD and one SA beam, highlighting the impact of hardware impairments on the true pattern. As with PN beams in [11], these pattern offsets reduce MP algorithm performance.
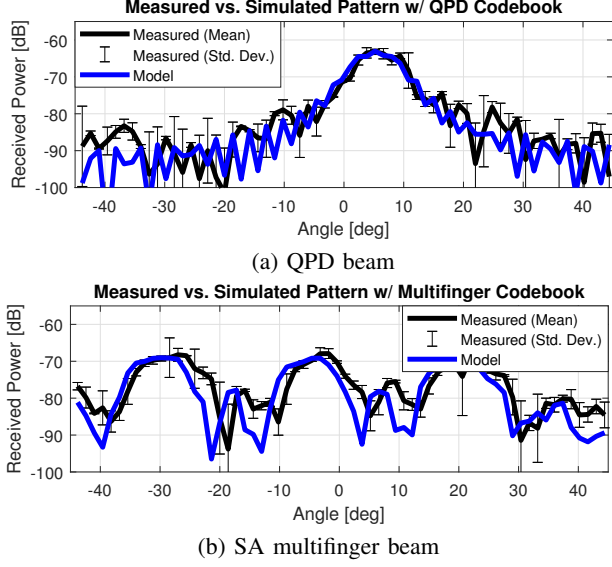
(a) QPD beam

(b) SA multifinger beam

Fig. 5: Theoretical (blue) and measured (black) beam patterns.

(a) Algorithms using only PN beams.

(b) Algorithms using 1 PN beam and the rest as SA beams.
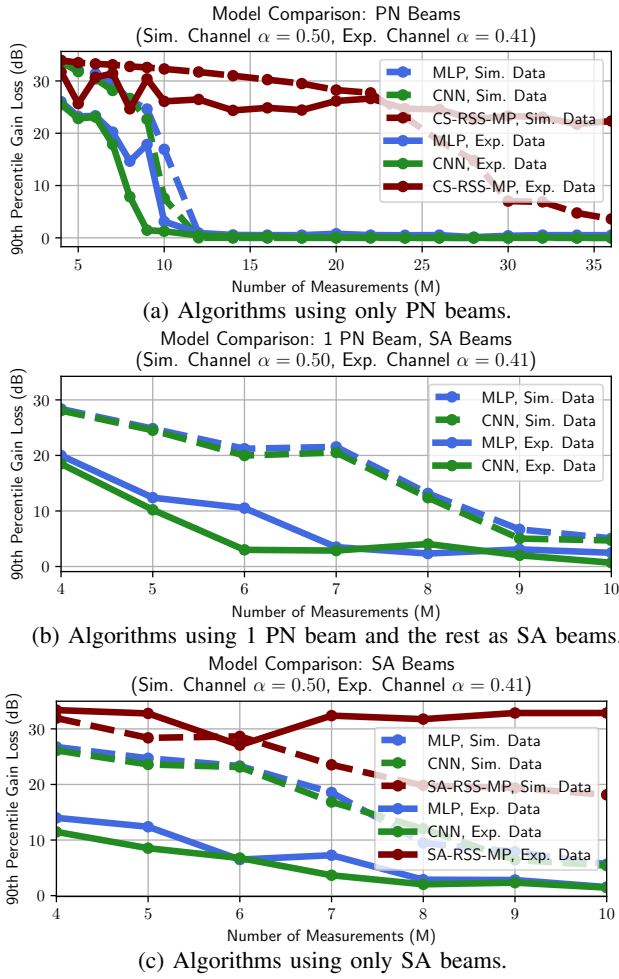

(c) Algorithms using only SA beams.

Fig. 6: Prediction algorithms under strong NLOS AoAs.

1) Beam Design Impact: The BA gain loss of $\mathbf{W}_s$ designs is first compared with CNN prediction algorithms and two channel configurations. Fig. 7 provides this comparison for simulated and experimental results with weak and strong multipath components. As expected with wide angular support, exclusive use of PN beam features provides nearly the worst performance in all four tests. While QPD beams have much less angular support than PN beams, this lack of angular coverage also provides less information to predict AoAs and reduces BA performance. In most cases, the lowest gain loss was reported for measurement combinations with SA beams and a few PN beams.

2) Prediction Algorithm Comparison: The prediction models were then compared to determine the best $p(\mathbf{y})$. Fig. 6 shows the comparison of CNN, MLP, and MP with three combinations of features. MP is used with the PN and SA codebooks to compare ML algorithms with previously described model-based methods. In all cases, the CNN algorithm provided the lowest gain loss, with order-of-magnitude reductions compared to MP algorithms and improvements ranging from 0 to 20 dB compared to the MLP algorithm. While the experimental and simulation results are superimposed, each dataset studies separate system parameters. Experiments show larger gain loss improvements in using ML methods over MP due to array impairments. Additionally, multipath forces the ML algorithms to learn from both the impact of hardware impairment and the training data channels. Thus, experimental results, with fewer combinations of path AoAs and gains, show better performance than simulations.

3) Required Number of Measurements: Based on the prior results, the best algorithm combination uses a combination of PN and SA beams for $\mathbf{W}_s$ and the CNN for $p(\mathbf{y})$. Fig. 8 compares the required number of measurements for the proposed algorithm combinations, mmRAPID, and PN-RSS-MP. Note that SA-RSS-MP is not included, as the algorithm did not sufficiently reduce the gain loss with the 10 beams used. The best combination, the CNN with 1 or 2 PN beams and SA beams, significantly decreases the BA communications overhead. While an exhaustive search would require $K = 51$ measurements in experiments, the best algorithm only requires 6, reducing overhead by 88%. PN-RSS-MP does not meet gain loss requirements with even 36 measurements in the strongest multipath channels and requires 16 in the best experimental case, demonstrating that the best algorithm reduces overhead by 63% or more. Compared to mmRAPID's 8 or 9 required measurements in experiments, the best algorithm still reduces overhead by over 25%. The proposed algorithm's benefits vary more in simulations, but still present significant performance improvements in all cases.
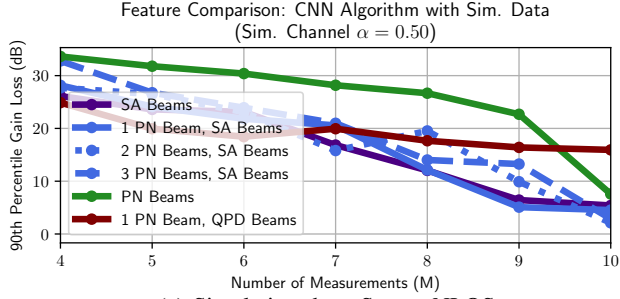
V. CONCLUSION AND FUTURE WORK

This paper proposes a novel phase-less UE BA algorithm for multipath channels, using a mixed beam design codebook and a CNN architecture. The design optimizes the heuristic codebook by empirically finding a balance between the sparse angular support required for phase-less prediction and the
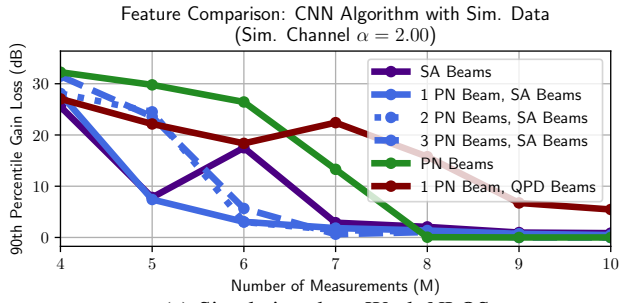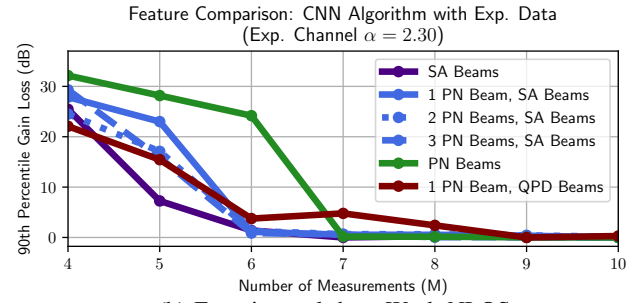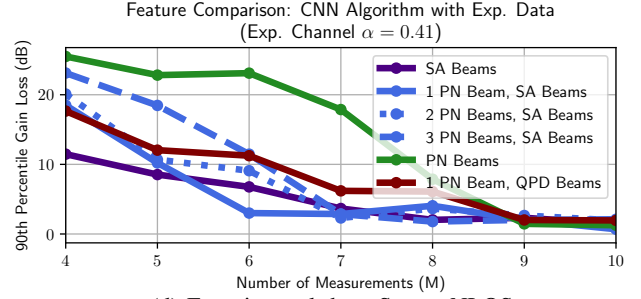
Fig. 7: Comparison of beam designs between simulations (Sim.) and experiments (Exp.) with strong and weak NLOS AoAs.
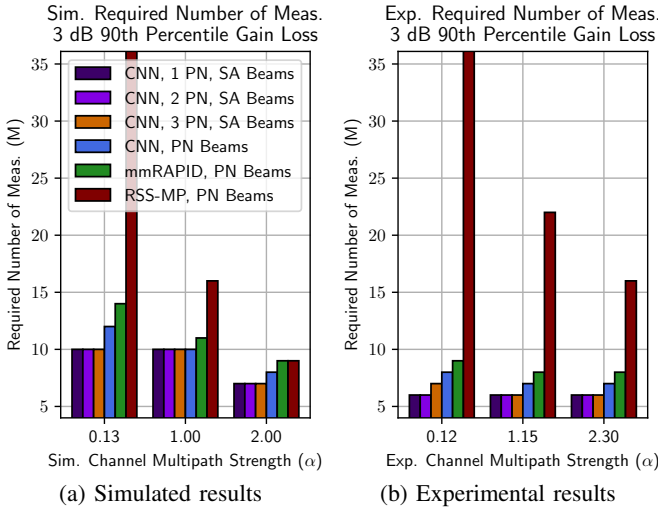
Fig. 8: Comparison of the required number of measurements to meet a 3 dB 90th percentile maximum required gain loss.

omnidirectionality required for a minimal number of measurements. The CNN architecture takes advantage of the feature space correlation of these beam designs. Using 1 or 2 PN beams and SA beams significantly reduces the required number of measurements for effective BA, demonstrating 88% and at least 63% less overhead in mmW experiments as compared to an exhaustive search and MP methods respectively.

The AoA prediction method and beam design in this work warrant future improvement. Improving the algorithm to predict multiple best AoAs could be helpful for backup connection beams in case of blockage. Additionally, a more comprehensive study of theoretically optimal sounding beam designs for phase-less BA has not yet been explored.

REFERENCES

[1] H. Hassanieh *et al.*, "Fast millimeter wave beam alignment," in *Proc. of the 2018 Conf. of the ACM Special Interest Group on Data Commun.*, Budapest, Hungary, Aug. 2018, p. 432–445.

[2] S. Noh, M. D. Zoltowski, and D. J. Love, "Multi-resolution codebook and adaptive beamforming sequence design for millimeter wave beam alignment," *IEEE Trans. Wireless Commun.*, vol. 16, no. 9, pp. 5689–5701, Sep. 2017.

[3] Y. Heng and J. G. Andrews, "Machine learning-assisted beam alignment for mmwave systems," in *2019 IEEE Global Commun. Conf. (GLOBECOM)*, 2019, pp. 1–6.

[4] M. Alrabeiah and A. Alkhateeb, "Deep learning for mmwave beam and blockage prediction using sub-6 ghz channels," *IEEE Trans. Commun.*, vol. 68, no. 9, pp. 5504–5518, Sep. 2020.

[5] V. Boljanovic *et al.*, "Design of millimeter-wave single-shot beam training for true-time-delay array," in *2020 IEEE 21st Int. Workshop on Signal Process. Advances in Wireless Commun. (SPAWC)*, 2020, pp. 1–5.

[6] H. Yan and D. Cabric, "Compressive initial access and beamforming training for millimeter-wave cellular systems," *IEEE J. of Select. Topics in Signal Process.*, vol. 13, no. 5, pp. 1151–1166, Sep. 2019.

[7] M. E. Rasekh *et al.*, "Noncoherent mmwave path tracking," in *Proc. of the 18th Int. Workshop on Mobile Computing Systems and Applicat.*, Sonoma, CA, USA, Feb. 2017, p. 13–18.

[8] X. Li *et al.*, "Fast beam alignment for millimeter wave communications: A sparse encoding and phaseless decoding approach," *IEEE Trans. Signal Process.*, vol. 67, no. 17, p. 4402–4417, Sep 2019.

[9] M. Polese, F. Restuccia, and T. Melodia, "DeepBeam: Deep Waveform Learning for Coordination-Free Beam Management in mmWave Networks," *arXiv:2012.14350 [cs, math]*, Dec. 2020.

[10] W. Ma, C. Qi, and G. Y. Li, "Machine learning for beam alignment in millimeter wave massive mimo," *IEEE Wireless Commun. Letters*, vol. 9, no. 6, pp. 875–878, Jun. 2020.

[11] H. Yan, B. W. Domae, and D. Cabric, "Mmrapid: Machine learning assisted noncoherent compressive millimeter-wave beam alignment," in *Proc. of the 4th ACM Workshop on Millimeter-Wave Networks and Sensing Syst.*, London, United Kingdom, Sep. 2020, pp. 1–6.

[12] T. S. Cousik *et al.*, "Fast Initial Access with Deep Learning for Beam Prediction in 5G mmWave Networks," *arXiv:2006.12653 [cs, eess]*, Jun. 2020.

[13] Y. Ghasempour *et al.*, "Multi-user multi-stream mmwave wlans with efficient path discovery and beam steering," *IEEE J. Sel. Areas Commun.*, vol. 37, no. 12, pp. 2744–2758, Dec 2019.

[14] M. R. Akdeniz *et al.*, "Millimeter wave channel modeling and cellular capacity evaluation," *IEEE J. Sel. Areas Commun.*, vol. 32, no. 6, pp. 1164–1179, Jun. 2014.

[15] S. Bicais and J.-B. Dore, "Phase noise model selection for sub-thz communications," in *2019 IEEE Global Commun. Conf. (GLOBECOM)*, 2019, pp. 1–6.

[16] K. H. Sayidmarie and Q. H. Sultan, "Synthesis of wide beam array patterns using quadratic-phase excitations," *Int. J. of Electromagnetics and Applicat.*, vol. 3, no. 5, pp. 127–135, 2013.